



Cite this: *Metallomics*, 2020, 12, 470

Received 7th December 2019,  
 Accepted 18th February 2020

DOI: 10.1039/c9mt00299e

rsc.li/metallomics

**N-Truncated  $A\beta_{4-42}$  displays a high binding affinity with  $Cu^{II}$ . A mechanistic scheme of the interactions between  $A\beta_{4-42}$  and  $Cu^{II}$  has been proposed using a fluorescence approach. The timescales of different conversion steps were determined. This kinetic mechanism indicates the potential synaptic functions of  $A\beta_{4-42}$  during neurotransmission.**

The amyloid- $\beta$  ( $A\beta$ ) peptides associated with Alzheimer's Disease (AD) comprise a number of species. The "canonical"  $A\beta_{1-42}$  and  $A\beta_{1-40}$  peptides derived directly by proteolysis of the Amyloid Precursor Protein (APP) are complemented by N- and C-truncated species, yielded by a variety of brain proteases.<sup>1</sup> Among them, the N-truncated  $A\beta_{4-42}$  has been reported as particularly abundant in the hippocampus and cortex of sporadic AD patients, as well as in healthy controls,<sup>2,3</sup> even exceeding  $A\beta_{1-42}$  and  $A\beta_{1-40}$ .<sup>4,5</sup>  $A\beta_{1-x}$  peptides can bind  $Cu^{II}$  using the N-terminus and H6, H13, and His14 residues.<sup>6-8</sup> Hence,  $A\beta_{1-16}$  has been adopted as a common model peptide in metal binding studies.  $K_d$  in the range of 0.1 nM to 1 nM at pH 7.1–7.4 was determined for  $A\beta_{1-16}$  and  $A\beta_{1-40}$ .<sup>9-11</sup> The adventitious binding of  $Cu^{II}$  ions to  $A\beta_{1-42/40}$  and the concomitant generation of reactive oxygen species (ROS) *via* the  $Cu^{II}/Cu^I$  redox pair has been proposed to be the molecular basis of oxidative stress and neuronal death in AD.<sup>12</sup> On the other hand,  $A\beta_{4-x}$  peptides bind a  $Cu^{II}$  ion more than three orders of magnitude more strongly ( $K_d = 30$  fM and 6.6 fM at pH 7.4 for  $A\beta_{4-16}$  and  $A\beta_{4-9}$ , respectively), using their N-terminal ATCUN motif spanning the Phe4, Arg5 and His6 residues. These complexes are redox-inert and do not generate significant ROS.  $Cu^{II}$  ion transfer from  $A\beta_{1-16}$  to  $A\beta_{4-16}$  occurs upon adding the latter to the  $Cu^{II}A\beta_{1-16}$  solution.<sup>13</sup>

## Hierarchical binding of copper<sup>II</sup> to N-truncated $A\beta_{4-16}$ peptide†

Xiangyu Teng,<sup>‡</sup> Ewelina Stefaniak,<sup>‡</sup> Paul Girvan,<sup>‡</sup> Radostaw Kotuniak,<sup>‡</sup> Dawid Płonka,<sup>‡</sup> Wojciech Bal,<sup>‡</sup> and Liming Ying<sup>‡</sup>

### Significance to metallomics

N-Truncated  $A\beta_{4-x}$  is abundant in both healthy and AD brains. Its  $Cu(II)$  binding affinity is three orders of magnitude stronger than well-known  $A\beta_{1-42}$  or  $A\beta_{1-40}$ . Using a model peptide,  $A\beta_{4-16}$ , we have elucidated the reaction mechanism of  $Cu(II)$  with  $A\beta_{4-x}$ , crucial to understand the physiological role and toxicity of  $A\beta$  peptides. The presence of two kinetic intermediates prior to the formation of the tight ATCUN complex has implications for the potential function of  $A\beta_{4-42}$  as a  $Cu(II)$  transporter during neurotransmission. The methodology used in this work may also stimulate the research of  $Cu(II)$  interactions with other intrinsically disordered proteins (IDPs).

This reaction is quantitative, in agreement with the affinity difference, and fast, occurring within the sample preparation time  $\sim$ s. Such a reaction suggested that  $A\beta_{4-42}$  should prevail as a  $Cu^{II}$  binding  $A\beta$  species in the extracellular spaces of the brain. This finding gave rise to a hypothesis that  $A\beta_{4-42}$  may have a physiological role as a synaptic  $Cu^{II}$  scavenger during neurotransmission.<sup>14</sup> However,  $Cu^{II}$  release events in glutamatergic synapses may occur on a much faster, millisecond scale. Therefore, a thorough determination of association and dissociation rate constants for the participating species is necessary to help evaluate their relevance *in vivo*. Such data have been obtained previously for  $Cu^{II}A\beta_{1-x}$  complexes.<sup>15-17</sup> Here, we studied the reaction mechanism for  $Cu^{II}$  binding to the model peptide  $A\beta_{4-16}$  and found that the reaction follows a hierarchical fashion, going through two intermediate states and then reaching the final tight complex.

First, we studied the effect of N-truncation on the  $Cu^{II}$  binding kinetics. 20 nM  $A\beta$  labelled by HiLyte Fluor 488 on lysine 16 (FRHDSGYEVHHQK-HiLyte 488) was reacted with 400 nM  $Cu^{II}$  under various HEPES concentrations in order to obtain the HEPES-independent  $Cu^{II}$  binding rate constant ( $k_{on}$ ). The results are shown in Fig. 1a. The intercept of the fitted curve (Fig. 1b) was used to determine  $k_{on}$ , which is  $2.0(1) \times 10^8 M^{-1} s^{-1}$ , 2.5 times slower than the value for  $A\beta_{1-16}$ .<sup>17</sup>

$k_{off}$  was determined for the reaction of a  $Cu^{II}$  complex of unlabelled  $A\beta_{4-16}$  with an excess of EDTA. The estimated value

<sup>a</sup> Department of Chemistry, Imperial College London, Molecular Sciences Research Hub, White City Campus, London W12 0BZ, UK

<sup>b</sup> Institute of Biochemistry and Biophysics, Polish Academy of Sciences, Pawińskiego 5a, 02-106 Warsaw, Poland. E-mail: wbal@ibb.waw.pl

<sup>c</sup> National Heart and Lung Institute, Imperial College London, Molecular Sciences Research Hub, White City Campus, London W12 0BZ, UK. E-mail: Lying@imperial.ac.uk

† Electronic supplementary information (ESI) available. See DOI: 10.1039/c9mt00299e

‡ These authors contributed equally to this work.



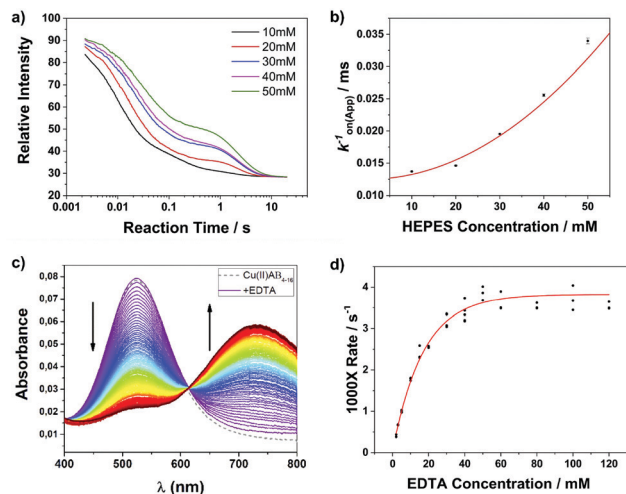


**Fig. 1** Kinetics of  $\text{Cu}^{\text{II}}$  binding to  $\text{A}\beta_{4-16}$ . (a) Representative raw traces of  $\text{A}\beta$  (20 nM) with  $\text{Cu}^{\text{II}}$  (400 nM) under various concentrations of HEPES. The experiments were performed in 50 mM HEPES and 100 mM NaCl buffer solution at 298 K (pH 7.5). (b) HEPES dependence of  $k_{\text{on}}$ . The HEPES independent  $k_{\text{on}}$  value is  $2.0(1) \times 10^8 \text{ M}^{-1} \text{ s}^{-1}$ . (c) Kinetics of dissociation of  $\text{Cu}^{\text{II}}\text{A}\beta_{4-16}$  assisted by varying concentrations of EDTA, monitored by UV-vis absorbance. The experiments were performed for 1 mM  $\text{Cu}^{\text{II}}\text{A}\beta_{4-16}$  at 298 K (pH 7.5). (d) Empirical fit to derive the EDTA-independent  $k_{\text{off}}$ .

is  $\sim 5 \times 10^{-5} \text{ s}^{-1}$ , which divided by  $k_{\text{on}}$  proposed here gives  $K_{\text{d}} \sim 250 \text{ fM}$ . EDTA is a stronger  $\text{Cu}^{\text{II}}$  chelator than  $\text{A}\beta_{4-16}$ , with a  $\log \beta$  of 18.7, which can be recalculated into a conditional constant  ${}^{\text{C}}K$  of 16.0 at pH 7.5.<sup>18</sup> This value is sufficiently higher than that of  $\text{Cu}^{\text{II}}\text{A}\beta_{4-16}$ , 13.53, to assure full  $\text{Cu}^{\text{II}}$  transfer, as demonstrated in Fig. 1c. The reaction was carried out for a range of EDTA/peptide ratios between 2 and 120. Pseudo-1st order kinetics for the  $\text{Cu}^{\text{II}}$  transfer reaction was observed for all experiments. The non-linear response of  $k_{\text{off}}$  to EDTA required the EDTA-independent  $k_{\text{off}}$  value to be determined by the extrapolation of the empirical exponential fit to these data, as shown in Fig. 1d.

To gain a glimpse of a possible reaction mechanism of  $\text{Cu}^{\text{II}}$  binding to N-truncated  $\text{A}\beta_{4-16}$ , we performed binding experiments at a 1:1 mixing ratio of  $\text{A}\beta$  to  $\text{Cu}^{\text{II}}$  with increasing concentration. In such experiments, the effect of the second  $\text{Cu}^{\text{II}}$  binding can be ignored, as the relevant  $\log K$  is as low as 6.7.<sup>13</sup> The raw traces are shown in Fig. 2a. We noticed that the reaction process is becoming concentration independent after  $\sim 2 \text{ s}$  (results from the fit are summarized in Table S1, ESI†). Thus we infer the existence of an intramolecular process following the initial  $\text{Cu}^{\text{II}}$  binding.

Next, a double mixing stopped flow technique was employed to further explore the potential intermediate complexes formed after the initial  $\text{Cu}^{\text{II}}$  binding. This technique was successfully applied to probe the interconversion between component I and component II  $\text{Cu}^{\text{II}}$  coordination species of  $\text{A}\beta_{1-16}$  and  $\text{A}\beta_{1-40}$ .<sup>17</sup>  $2 \mu\text{M}$   $\text{A}\beta_{4-16}$  and  $2 \mu\text{M}$   $\text{Cu}^{\text{II}}$  were mixed in a delay loop and after various delay times the reaction was “frozen” by adding an excess of EDTA (Fig. 2b). Taking advantage of the disparities in reactivity of different  $\text{Cu}^{\text{II}}\text{A}\beta_{4-16}$  species with EDTA, the time evolution of the population of individual species could be

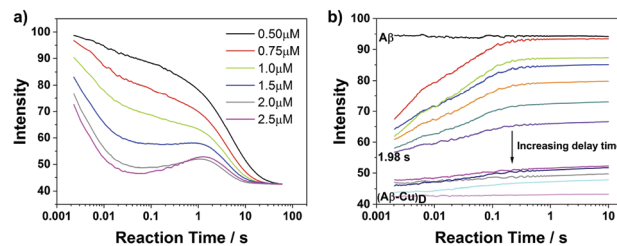


**Fig. 2** (a) Raw traces of  $\text{Cu}^{\text{II}}$  binding measurements with a series of 1:1 concentration ratio HiLyte 488 labelled  $\text{A}\beta$  and  $\text{Cu}^{\text{II}}$  showing the evidence of intermediate species formation. The experiment was performed in 50 mM HEPES and 100 mM NaCl buffer solution at 298 K (pH 7.5). (b) Kinetics of HiLyte 488 labelled  $\text{A}\beta/\text{Cu}^{\text{II}}$  interactions measured by double mixing stopped flow. Raw traces showing the change in amplitude as the delay time between mixing of an equal concentration of  $\text{Cu}^{\text{II}}$  and  $\text{A}\beta$  (2  $\mu\text{M}$ ) and addition of EDTA is increased from 50 ms to 1 min. The experiment was performed in 50 mM HEPES and 100 mM NaCl buffer solution at 298 K (pH 7.5).

resolved and analyzed, enabling us to depict details of the binding process.

As shown in Fig. 2b, the amplitude of fluorescence recovery strongly depends on the delay time, indicating that a much more inert (less reactive towards EDTA) complex (“dark” complex) formed after around 2 s. We equate this end complex,  $(\text{A}\beta\text{-Cu})_{\text{D}}$ , to the very stable ATCUN-type  $\text{Cu}^{\text{II}}\text{A}\beta_{4-16}$  complex reported previously.<sup>13</sup> Furthermore, because the reaction rate is concentration independent after 2 s as mentioned above, we propose that a peptide conformational rearrangement process leading to this final complex must occur at around 2 s.

In order to describe the whole process of  $\text{Cu}^{\text{II}}$  binding of N-truncated  $\text{A}\beta_{4-16}$ , we hypothesized a reaction scheme as shown in Fig. 3a. The individual amplitudes of the two phases in Fig. 2b were determined by a global fit, which were further fitted by the scheme with KinTek software to validate it (Fig. 3b). The amplitudes indicate the amounts of two intermediates, Species I and Species II, at different reaction process stages, and could be

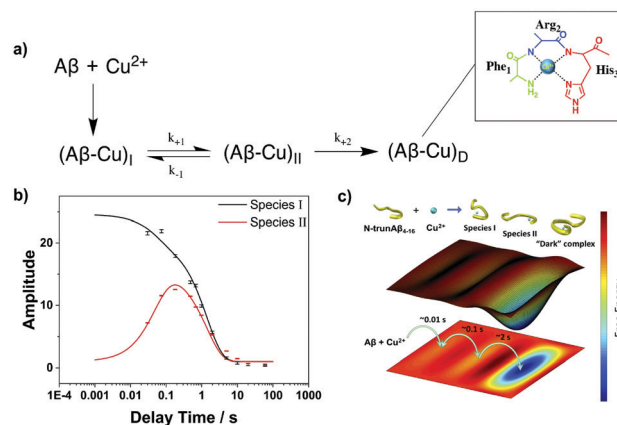


**Fig. 3** (a) Reaction mechanism of  $\text{Cu}^{\text{II}}$  binding to  $\text{A}\beta_{4-16}$  and formation of the high affinity  $\text{Cu}^{\text{II}}\text{A}\beta_{4-16}$  complex,  $(\text{A}\beta\text{-Cu})_{\text{D}}$  ( $\text{Cu}^{\text{II}}$  binding site shown above). (b) Fitting of the individual amplitudes at different  $\text{Cu}^{\text{II}}$  binding process stages of the two phases by the predicted reaction mechanism. (c) Proposed free energy landscape of  $\text{Cu}^{\text{II}}$  binding to  $\text{A}\beta_{4-16}$ . “Dark” complex refers to the very stable ATCUN-type  $\text{Cu}^{\text{II}}\text{A}\beta_{4-16}$  complex.



**Table 1** Rate constants corresponding to the mechanism scheme shown in Fig. 3a

	$k_{+1}$	$k_{-1}$	$k_{+2}$
$k$ value/s <sup>-1</sup>	4.10(1)	10.34(2)	3.31(4)

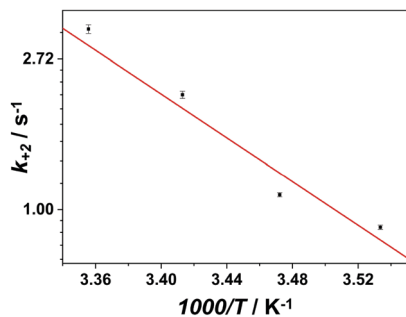


**Fig. 4** Arrhenius plot for the switching rate constant  $k_{+2}$ . The switching activation energy determined is 64(3) kJ mol<sup>-1</sup>.

fitted well by the predicted mechanism, with fitted rate constants listed in Table 1. A corresponding free energy landscape illustration of Cu<sup>II</sup> binding with A $\beta$ <sub>4-16</sub> is shown in Fig. 3c.

Finally, the activation energy of the (A $\beta$ -Cu)<sub>D</sub> complex was determined to be 64(3) kJ mol<sup>-1</sup> (Fig. 4) by performing a series of double mixing experiments at different temperatures (raw data shown in Fig. S1, ESI<sup>†</sup>).

The chemical properties of ATCUN Cu<sup>II</sup> complexes of A $\beta$ <sub>4-x</sub> peptides, such as high thermodynamic stability, absence of ROS production due to their resistance to oxidation and reduction, reluctance of copper to transfer to metallothionein-3 (MT3) and easy sequestering of Cu<sup>II</sup> from A $\beta$ <sub>1-x</sub>, gave rise to a concept that A $\beta$ <sub>4-x</sub> peptides (full-length A $\beta$ <sub>4-42</sub> and its C-truncated analogs) may serve as guardians of synaptic function, by sequestering excess Cu<sup>II</sup> ions released during neurotransmission in glutamatergic pathways.<sup>14,19</sup> The key unsolved issue is how these exchange-inert complexes relay copper back to neurons to maintain the proper copper cycling. Furthermore, Cu<sup>II</sup>-free A $\beta$ <sub>4-42</sub> can be neurotoxic by forming oligomeric species.<sup>20</sup> Detailed knowledge on mechanisms of Cu<sup>II</sup> association with and dissociation from A $\beta$ <sub>4-x</sub> peptides, represented here by A $\beta$ <sub>4-16</sub>, is thus crucial to understand the physiology and toxicity of these A $\beta$  peptides.

The discovery of long-lived kinetic intermediates in the formation of the ATCUN complex of A $\beta$ <sub>4-16</sub> is a game changer in the above considerations. The lifetimes of Species I and Species II complexes are comparable to the intervals between pulses of neurotransmitter release in glutamatergic neuronal pathways.<sup>21</sup> Therefore, these complexes may well contribute to the biological activity of A $\beta$ <sub>4-42</sub>, and of putative short peptidic fragments generated by neprilysin cleavage, such as A $\beta$ <sub>4-9</sub>.<sup>22,23</sup> There is only one way in which four nitrogen ligands of the ATCUN motif can be arranged around the Cu<sup>II</sup> ion, and so it is reasonable to assume that the intermediate species contain the coordinatively unsaturated Cu<sup>II</sup>. Such species have been implicated in the reverse reaction of Cu<sup>II</sup> dissociative transfer from Cu<sup>II</sup>A $\beta$ <sub>4-16</sub> to MT3, to explain the catalytic effect of glutamate,<sup>24</sup>

but it has not been observed directly. The Species I and in particular the longer-lived Species II complex may be the actual species able to move copper around during neurotransmission. The fact that the Cu<sup>II</sup>A $\beta$ <sub>1-x</sub> complex, although so much weaker, was formed 2.5 times faster, prompts further research into possible synaptic roles of Cu<sup>II</sup> interactions with various A $\beta$  species.

Furthermore, the observed hierarchical binding of Cu<sup>II</sup> to A $\beta$ <sub>4-16</sub> resembles the kinetics of the binding of many intrinsically disordered proteins (IDPs).<sup>25</sup> The methodology used in this study may be applicable to the fundamental understanding of the emerging “coupled binding and folding” paradigm.<sup>26</sup>

## Conflicts of interest

There are no conflicts to declare.

## Acknowledgements

This work was supported by the Leverhulme Trust grant RPG-2015-345 to LY and the Biotechnology and Biosciences Research Council (UK) grant BB/R022429/1 to LY, and the National Science Centre in Poland: PRELUDIUM Grant No. 2016/21/N/NZ1/02785 and ETIUDA Grant No. 2018/28/T/NZ1/00452, to ES, and OPUS Grant No. 2018/29/B/ST4/01634 to WB. The equipment used was sponsored in part by the Centre for Preclinical Research and Technology (CePT) under award number POIG.02.02.00-14-024/08-00, a project co-sponsored by European Regional Development Fund and Innovative Economy, the National Cohesion Strategy of Poland.

## Notes and references

- 1 D. J. Selkoe, *Physiol. Rev.*, 2001, **81**, 741–766.
- 2 C. L. Masters, G. Simms, N. A. Weinman, G. Multhaup, B. L. McDonald and K. Beyreuther, *Proc. Natl. Acad. Sci. U. S. A.*, 1985, **82**, 4245–4249.
- 3 E. Portelius, N. Bogdanovic, M. K. Gustavsson, I. Volkman, G. Brinkmalm, H. Zetterberg, B. Winblad and K. Blennow, *Acta Neuropathol.*, 2010, **120**, 185–193.
- 4 G. Antonios, N. Saiepour, Y. Bouter, B. C. Richard, A. Paetau, A. Verkoniemi-Ahola, L. Lannfelt, M. Ingelsson, G. G. Kovacs, T. Pillot, O. Wirths and T. A. Bayer, *Acta Neuropathol. Commun.*, 2013, **1**, 56.
- 5 T. A. Bayer and O. Wirths, *Acta Neuropathol.*, 2014, **127**, 787–801.
- 6 P. Dorlet, S. Gambarelli, P. Faller and C. Hureau, *Angew. Chem.*, 2009, **121**, 9437–9440 (*Angew. Chem., Int. Ed.*, 2009, **48**, 9273–9276).
- 7 B. Alies, H. Eury, C. Bijani, L. Rechinat, P. Faller and C. Hureau, *Inorg. Chem.*, 2011, **50**, 11192–11201.
- 8 E. Atrián-Blasco, P. Gonzalez, A. Santoro, B. Alies, P. Faller and C. Hureau, *Coord. Chem. Rev.*, 2018, **375**, 38–55.
- 9 B. Alies, E. Renaglia, M. Rózga, W. Bal, P. Faller and C. Hureau, *Anal. Chem.*, 2013, **85**, 1501–1508.
- 10 T. R. Young, A. Kirchner, A. G. Wedd and Z. Xiao, *Metalloomics*, 2014, **6**, 505–517.



- 11 A. Conte-Daban, V. Borghesani, S. Sayen, E. Guillon, Y. Journaux, G. Gontard, L. Lisnard and C. Hureau, *Anal. Chem.*, 2017, **89**, 2155–2162.
- 12 C. Cheignon, M. Jones, E. Atrián-Blasco, I. Kieffer, P. Faller, F. Collin and C. Hureau, *Chem. Sci.*, 2017, **8**, 5107–5118.
- 13 M. Mital, N. E. Wezynfeld, T. Frączyk, M. Z. Wiloch, U. E. Wawrzyniak, A. Bonna, C. Tumpach, K. J. Barnham, C. L. Haigh, W. Bal and S. C. Drew, *Angew. Chem.*, 2015, **127**, 10606–10610 (*Angew. Chem., Int. Ed.*, 2015, **54**, 10460–10464).
- 14 E. Stefaniak and W. Bal, *Inorg. Chem.*, 2019, **58**, 13561–13577.
- 15 P. Girvan, T. Miyake, X. Teng, T. Branch and L. Ying, *ChemBioChem*, 2016, **17**, 1732–1737.
- 16 T. Branch, M. Barahona, C. A. Dodson and L. Ying, *ACS Chem. Neurosci.*, 2017, **8**, 1970–1979.
- 17 T. Branch, P. Girvan, M. Barahona and L. Ying, *Angew. Chem.*, 2015, **127**, 1243–1246 (*Angew. Chem., Int. Ed.*, 2015, **54**, 1227–1230).
- 18 J. Felcman and J. J. da Silva, *Talanta*, 1983, **30**, 565–570.
- 19 N. E. Wezynfeld, E. Stefaniak, K. Stachucy, A. Drozd, D. Płonka, S. C. Drew, A. Krężel and W. Bal, *Angew. Chem.*, 2016, **128**, 8375–8378 (*Angew. Chem., Int. Ed.*, 2016, **55**, 8235–8238).
- 20 J. Dunys, A. Valverde and F. Checler, *J. Biol. Chem.*, 2018, **293**, 15419–15428.
- 21 W. Goch and W. Bal, *PLoS One*, 2017, **12**, e0170749.
- 22 M. Mital, W. Bal, T. Frączyk and S. C. Drew, *Inorg. Chem.*, 2018, **57**, 6193–6197.
- 23 K. Bossak-Ahmad, M. Mital, D. Płonka, S. C. Drew and W. Bal, *Inorg. Chem.*, 2019, **58**, 932–943.
- 24 A. Santoro, N. Wezynfeld, E. Stefaniak, A. Pomorski, D. Płonka, A. Krężel, W. Bal and P. Faller, *Chem. Commun.*, 2018, **54**, 12634–12637.
- 25 K. Sugase, H. J. Dyson and P. E. Wright, *Nature*, 2007, **447**, 1021–1025.
- 26 S. Gianni, J. Dogan and P. Jemth, *Curr. Opin. Struct. Biol.*, 2016, **36**, 18–24.

